Fermilab FERMILAB-TM-2196 March 2003

Muon Cooling Channels*

Eberhard Keil

November 26, 2002

Abstract

A procedure uses the equations that govern ionization cooling, and leads to the most important parameters of a muon cooling channel that achieves assumed performance parameters. First, purely transverse cooling is considered, followed by both transverse and longitudinal cooling in quadrupole and solenoid channels. Similarities and differences in the results are discussed in detail, and a common notation is developed. Procedure and notation are applied to a few published cooling channels. The parameters of the cooling channels are derived step by step, starting from assumed values of the initial, final and equilibrium emittances, both transverse and longitudinal, the length of the cooling channel, and the material properties of the absorber. The results obtained include cooling lengths and partition numbers, amplitude functions and limits on the dispersion at the absorber, length, aperture and spacing of the absorber, parameters of the RF system that achieve the longitudinal amplitude function and bucket area needed. Finally, I compute the merit factor that describes the enhancement of the density in 6D phase space. The consequences of changes in the input parameters are discussed. The lattice parameters needed to achieve the assumed performance are summarised. The design proper of such a lattice, i.e. finding the precise arrangement of magnets, RF cavities, absorbers, etc., which has these properties is well beyond the scope of this document.

1 INTRODUCTION

In this document, I develop a procedure in the form of a *Mathematica* notebook, which leads to the most important parameters of a muon cooling channel that achieves assumed performance parameters. I first assemble the equations that govern ionization cooling. In Chapter 2, I consider purely transverse cooling, following [1]. In Chapter 3, I treat both transverse and longitudinal cooling in styles due to Neuffer [2] and Wang and Kim [3]. I discuss the similarities and discrepancies in their results in detail, and develop my own notation. In Chapter 4, I apply my procedure and notation to a few published cooling channels. In Chapter 5, I derive the parameters of the cooling channels step by step. I start from assumed values of the initial, final and equilibrium emittances, both transverse and longitudinal, the length of the cooling channel, and the material properties of the absorber. I obtain cooling lengths and partition numbers, amplitude functions and limits on the

*Operated by Universities Research Association Inc. under Contract No. DE-AC02-76CH03000 with the United States Department of Energy.

dispersion at the absorber, length, aperture and spacing of the absorber, parameters of the RF system that achieve the longitudinal amplitude function and bucket area needed. Finally, I compute the merit factor that is meaningful only if muon losses along the channel for reasons other than muon decay are negligible compared to the decay losses. In Chapter 6, I discuss the consequences of changes in the input parameters, and summarise the lattice parameters needed to achieve the assumed performance. The design proper of such a lattice, i.e. finding the precise arrangement of magnets, RF cavities, absorbers, etc., which has these properties is well beyond the scope of this document. My conclusions are in Chapter 7.

In the following a muon cooling channel may be either an open transport line or one or more turns in a cooling ring.

2 TRANSVERSE COOLING

A typical channel for reducing the transverse normalised emittance of the muon beam consists of liquid hydrogen targets in which the muon beam is decelerated and its normalised emittance reduced, and of RF cavities that compensate the average energy loss in the targets. Between the targets, the muon beam is focused, typically by solenoids that are arranged such that the amplitude function $\beta_\perp$ has a minimum at the targets. We arrive at the following differential equation for the normalised transverse emittance $\varepsilon_\perp$ with the negative cooling term from ionization and the positive heating term from Coulomb scattering [1]:

$$\frac{\mathrm{d}\varepsilon_\perp}{\mathrm{d}s} = -\frac{\varepsilon_\perp}{\beta^2 E}\frac{\mathrm{d}E}{\mathrm{d}s} + \frac{\beta_\perp (13.6\ \mathrm{MeV})^2}{2\beta^3 E_\mu X_0 E} \tag{1}$$

Here E is the total and E_μ the rest energy of the muon, β and γ are the associated relativistic factors; $\mathrm{d}E/\mathrm{d}s$ is the rate of energy loss in the hydrogen target, X_0 is its radiation length. All quantities in (1) may be functions of the distance s along the cooling channel. Both $\mathrm{d}\varepsilon_\perp/\mathrm{d}s$ and $1/X_0$ are non-zero in the absorbers, and vanish elsewhere. The muon energy E, β and γ decrease in the absorbers, and increase in the RF cavities.

We gain some insight by averaging all these quantities along the cooling channel. I postpone the discussion of the exact meaning of averaging until Section 3.2, and don't bother to put bars above quantities or <> signs around them. We notice that cooling stops at the equilibrium emittance $\varepsilon_\perp^{eq}$, that we find by putting $\mathrm{d}\varepsilon_\perp/\mathrm{d}s = 0$ above and solving for $\varepsilon_\perp$:

$$\varepsilon_\perp^{eq} = \left(\frac{\mathrm{d}E}{\mathrm{d}s}\right)^{-1} \frac{\beta_\perp (13.6\ \mathrm{MeV})^2}{2\beta E_\mu X_0} \tag{2}$$

In order to obtain a small $\varepsilon_\perp$, we want an absorber with a large product $X_0 \frac{\mathrm{d}E}{\mathrm{d}s}$ of radiation length X_0 and energy loss $\frac{\mathrm{d}E}{\mathrm{d}s}$ in an optical arrangement with small $\beta_\perp$ at the absorber. By averaging the s-dependent quantities in (1) we turn it into a first-order differential equation with constant coefficients that we can solve in closed form:

$$\varepsilon_\perp(s) = \varepsilon_\perp^{eq} + (\varepsilon_\perp^{i} - \varepsilon_\perp^{eq}) \exp(-s/s_\perp^c) \tag{3}$$

Here $s_\perp^c = \beta^2 E/(\mathrm{d}E/\mathrm{d}s)$ is the transverse cooling length, and $\varepsilon_\perp^i$ is the initial normalised transverse emittance at $s = 0$, and $\varepsilon_\perp \to \varepsilon_\perp^{eq}$ for $s \to \infty$ as expected. In order to achieve an enhancement at all of the transverse phase space density of the muons in a cooling channel, the cooling

length $s_\perp$ must be short compared to the muon decay length $s_d = \beta\gamma c\tau_\mu$, where τ_μ is the muon lifetime at rest. Tab. 1 shows the effect of the equilibrium emittance $\varepsilon_\perp^{eq}$ on the length of a cooling channel that reduces $\varepsilon_\perp$ by a factor e. For $\varepsilon_\perp^{eq} \to 0$, we have $s/s_\perp \to 1$.

Table 1: Scaled length $s/s_\perp^c$ of a cooling channel that reduces the normalised transverse emittance by a factor e as a function of the ratio $\varepsilon_\perp^f/\varepsilon_\perp^{eq}$ of final and equilibrium emittance.

$\varepsilon_\perp^f/\varepsilon_\perp^{eq}$	2	3	5	10	20	50	100
$s/s_\perp^c$	1.489	1.275	1.1467	1.0679	1.0327	1.0128	1.0064

A common figure of merit M for a cooling channel is the product of the three ratios of initial over final emittance in the x, y and s directions, multiplied by an exponential factor describing the muon decay in the channel with decay time at rest $\tau_\mu = 2.19703\ \mu$s and decay length $c\tau_\mu = 658.654$ m:

$$M = \frac{\varepsilon_x^0}{\varepsilon_x^f}\frac{\varepsilon_y^0}{\varepsilon_y^f}\frac{\varepsilon_s^0}{\varepsilon_s^f}\exp\left(-\frac{s}{\beta\gamma c\tau_\mu}\right) \tag{4}$$

M is meaningful only if muon losses along the channel due to reasons other than muon decay are negligible compared to the decay losses.

3 TRANSVERSE AND LONGITUDINAL COOLING

We now apply the same recipe to cooling channels that cool muon beams both transversely and longitudinally. A small amount of longitudinal cooling is already present in a typical channel for transverse cooling, if the energy loss $\mathrm{d}E/\mathrm{d}s$ is an increasing function of E within the range of muon energies. This is the case if the muon momenta are larger than about 300 MeV/c. In practice, longitudinal cooling is typically done by wedge-shaped absorbers installed where muons of different momenta are transversely separated by having non-zero dispersion D at the absorber.

3.1 Neuffer Style

Neuffer has given the differential equations for transverse and longitudinal cooling [2]. His style works for cooling channels with observation points outside the solenoid focusing fields. His equation for the normalised transverse emittance $\varepsilon_\perp$ is:

$$\frac{\mathrm{d}\varepsilon_\perp}{\mathrm{d}s} = -\frac{\varepsilon_\perp g_\perp}{\beta^2 E}\frac{\mathrm{d}E}{\mathrm{d}s} + \frac{\beta_\perp (13.6\ \mathrm{MeV})^2}{2\beta^3 E_\mu X_0 E} \tag{5}$$

The dimension of $\varepsilon_\perp$ is a length as in (1). The new factor $g_\perp = 1 - D\ell'/\ell_0$ is the transverse partition number analogous to the partition numbers in synchrotron radiation damping, ℓ'/ℓ_0 is the relative transverse rate of change of the absorber length, and ℓ_0 is the length of the absorber at vanishing energy error.

Neuffer's equation for the normalised longitudinal emittance $\varepsilon_\parallel$ in units of energy and phase (E, ϕ) is:

$$\frac{\mathrm{d}\varepsilon_\parallel}{\mathrm{d}s} = -\frac{\varepsilon_\parallel g_\parallel}{\beta^2 E}\frac{\mathrm{d}E}{\mathrm{d}s} + \frac{\beta_\parallel}{2}\frac{\mathrm{d}\langle\Delta E^2\rangle}{\mathrm{d}s} \tag{6}$$

The longitudinal partition number $g_\parallel$ consists of two parts, the first is due to the variation of $\mathrm{d}E/\mathrm{d}s$ with $\beta\gamma$, and vanishes in the neighbourhood of $\beta\gamma \approx 3$, the second is due to the wedge absorbers:

$$g_\parallel = \frac{2\gamma^2 - 2\ln[K(\gamma^2-1)]}{\gamma^2\ln[K(\gamma^2-1)] - (\gamma^2-1)} + \frac{D\ell'}{\ell_0} \tag{7}$$

Here $K = 2m_ec^2/I$, and m_ec^2 is the electron mass. The ionization potential is $I = 16Z^{0.9}$ eV, and Z is the atomic number. In a cooling ring with circumference C, slip factor η, muon energy E, harmonic number h, RF wavelength λ_{RF}, peak RF voltage V, average RF voltage gradient $V' = V/C$, and stable phase angle φ_s, counted from the last zero crossing (or from the last peak?), Neuffer defines the longitudinal amplitude function at the absorber $\beta_\parallel$ as follows:

$$\beta_\parallel^2 = \frac{2\pi\eta}{\beta^3\gamma eV'\lambda_{\mathrm{RF}}E_\mu\sin\varphi_s} \tag{8}$$

The dimension of $\beta_\parallel$ is the reciprocal of an energy. Section 3.4.1 discusses the relations between Neuffer's $\beta_\parallel$, Wang and Kim's β_L, β_s printed by MAD, and my calculation from first principles. Neuffer gives the following expression for the heating term due to straggling:

$$\frac{\mathrm{d}\langle\Delta E^2\rangle}{\mathrm{d}s} = 4\pi(r_e\gamma m_ec^2)^2n_e(1-\beta^2/2) \tag{9}$$

Here $n_e = N_A\rho Z/A$ is the electron density in the material, N_A is Avogadro's number, r_e the classical electron radius, ρ the density, A the atomic weight. The sum of the partition numbers over the two transverse and on longitudinal plane becomes:

$$\sum g = 2 - \frac{2\gamma^2 - 2\ln[K(\gamma^2-1)]}{\gamma^2\ln[K(\gamma^2-1)] - (\gamma^2-1)} \tag{10}$$

The fact that the wedge parameter $D\ell'/\ell_0$ does not appear suggests considering them partition numbers. A cooling channel cools both longitudinally and transversely if all partition numbers are positive. This implies that $0 \le D\ell'/\ell_0 \le 1$.

Having assembled all the pieces, we can proceed as in Chapter 2, and average all parameters appearing in (5) and (6) over s. The two equilibrium emittances and the two cooling lengths become:

$$\varepsilon_\perp^{eq} = \left(\frac{\mathrm{d}E}{\mathrm{d}s}\right)^{-1}\frac{\beta_\perp(13.6\ \mathrm{MeV})^2}{2\beta g_\perp E_\mu X_0} \tag{11}$$

$$\varepsilon_\parallel^{eq} = \left(\frac{\mathrm{d}E}{\mathrm{d}s}\right)^{-1}\frac{\beta^2E\beta_\parallel}{2g_\parallel}\frac{\mathrm{d}\langle\Delta E^2\rangle}{\mathrm{d}s} \tag{12}$$

$$s_\perp^c = \frac{\beta^2E}{g_\perp}\left\langle\frac{\mathrm{d}E}{\mathrm{d}s}\right\rangle^{-1} \tag{13}$$

$$s_\parallel^c = \frac{\beta^2E}{g_\parallel}\left\langle\frac{\mathrm{d}E}{\mathrm{d}s}\right\rangle^{-1} \tag{14}$$

The two cooling rates $1/s^c$ are in the ratio of the partition numbers. In a typical cooling channel with $g_\perp \approx g_\parallel \approx 1/2$, the transverse equilibrium emittance in (11) and the transverse cooling length

in (13) are both about a factor of two larger than those given earlier. The closed solutions for both transverse and longitudinal emittance have the form of (3) with the appropriate expressions for initial and equilibrium emittances, and cooling lengths, i.e.

$$\varepsilon(s) = \varepsilon^{eq} + (\varepsilon^0 - \varepsilon^{eq}) \exp(-s/s^c) \tag{15}$$

3.2 The Meaning of Averaging

So far, I have not been specific about the meaning of averaging. Let us look what happens when the absorber is diluted and made longer, perhaps up to the point where it occupies the whole cooling channel. The expressions (2) and (11) for transverse equilibrium emittances all contain the factor $(\mathrm{d}E/\mathrm{d}s)X_0$. This product remains the same when the absorber is diluted, since $\mathrm{d}E/\mathrm{d}s$ decreases while X_0 increases in the same proportion. Similarly, the longitudinal equilibrium emittance (12) is proportional to the ratio $(\mathrm{d}\langle\Delta E^2\rangle/\mathrm{d}s)/(\mathrm{d}E/\mathrm{d}s)$ in which both brackets are proportional to the absorber density. Hence, this ratio is also independent of the absorber dilution. I believe that the amplitude functions $\beta_\perp$ and $\beta_\parallel$ at the absorber should be used in (2), (11) and (12).

Since $\mathrm{d}E/\mathrm{d}s$ appears alone in the cooling lengths (13) and (14) it should be multiplied by the filling factor, i.e. the ratio of total absorber length over cooling channel length. Hence $\mathrm{d}E/\mathrm{d}s$ is enclosed in angular brackets in (13) and (14).

3.3 Wang and Kim Style

Wang and Kim used moment equations for a linear theory of ionization cooling in 6D phase space [3]. They argued that the changes of emittance within a period of the cooling channel are small, used averaging over the periods, and obtained equations for the equilibrium emittances and the cooling lengths. The cooling channel may contain drift spaces, solenoids, dipoles, quadrupoles, and RF cavities. In this section, the subscripts s and z mark the transverse and longitudinal motion, respectively.

I tried to solve their system of coupled equations (32) to (36), assuming that all coefficients are independent of s, so far without success, since *Mathematica* runs out of memory. However, their equation (36) for the longitudinal emittance ε_z is independent of the other four equations, and can be solved for $\varepsilon_z(s)$ in closed form with the cooling length $s_z = 1/(2ec_- + \partial_\delta \eta)$ and equilibrium emittance $\varepsilon_z^{eq} = \chi_z s_z$:

$$\varepsilon_z(s) = \varepsilon_{z0} \exp(-s/s_z) + \varepsilon_z^{eq} \left[1 - \exp(-s/s_z)\right] \tag{16}$$

This result has the same form as (15), and the desirable properties that $\varepsilon_z(0) = \varepsilon_{z0}$, the prescribed initial value, and that $\varepsilon_z \to \varepsilon_x^{eq}$ for $s \to \infty$. The result (16) for ε_z^{eq} agrees with (43) of Wang and Kim, apart from the fact that they write bars on top of their quantities and I don't.

Wang and Kim state that ε_a, ε_{xy} and ε_L are orders of magnitude smaller than ε_s and ε_z. Neglecting them in their equation (32) decouples it from the other three equations. It can be solved in closed form with cooling length $s_s = 1/(\eta - ec_-)$ and equilibrium emittance $\varepsilon_s^{eq} = \chi_s s_s$ with the result:

$$\varepsilon_s(s) = \varepsilon_{s0} \exp(-s/s_s) + \varepsilon_s^{eq} \left[1 - \exp(-s/s_s)\right] \tag{17}$$

This result also has the same form as (15), and the desirable properties that $\varepsilon_z(0) = \varepsilon_{z0}$, the prescribed initial value, and that $\varepsilon_z \to \varepsilon_x^{eq}$ for $s \to \infty$. The next step is linking the parameters in Wang and Kim notation to physical quantities.

$$
\begin{aligned}
e &= |\vec{D}| \cdot |\vec{\partial\eta}|/2 && (18)\\
c_- &= \cos(\theta_D - \theta_W) && (19)\\
\eta &= \frac{1}{pv}\frac{\mathrm{d}E}{\mathrm{d}s} && (20)\\
\chi_z &= \left[\beta_L \chi_\delta + \gamma_L (D_x^2 + D_y^2)\chi\right]/2 && (21)\\
\chi_s &= \left(\beta_T \chi + \mathcal{H}_s \chi_\delta\right)/2 && (22)\\
\chi &= \left(\frac{13.6\ \mathrm{MeV}}{pv}\right)^2 \frac{1}{X_0} && (23)\\
\mathcal{H}_s &= \left(\mathcal{H}_x + \mathcal{H}_y\right)/2 && (24)
\end{aligned}
$$

Here, θ_D and θ_W are the rotations of the dispersion vector and of the wedges. I see very good reasons for making them equal, and putting $c_- = 1$. The subscripted β and γ are the transverse and longitudinal amplitude functions; D_x and D_y are the two components of the dispersion vector $\vec{D}$; χ and $\chi_\delta = \langle\delta^2\rangle$ are the rates of change per unit length of the mean square transverse angles due to multiple scattering and of the mean square relative momentum error due to straggling, respectively. $\mathcal{H}_x$ and $\mathcal{H}_y$ are the usual functions $\mathcal{H}_a = \gamma_a D_a^2 + 2\alpha_a D_a D_a' + \beta_a D_a'^2$, where the subscript a is either x or y.

To simplify the notation, I assume that wedge absorbers whose length depends on the vertical coordinate y are installed in places where $D_x = 0$ and $D_y \neq 0$, as in Balbekov's ring cooler [6]. Using (18) to (24) and assuming $c_- = 1$, then yields for cooling lengths and equilibrium emittances:

$$
\begin{aligned}
s_s^{-1} &= \eta - e c_- = \frac{1}{pv}\left\langle \frac{\mathrm{d}E}{\mathrm{d}s} - \frac{D_y}{2}\frac{\partial}{\partial y}\left(\frac{\mathrm{d}E}{\mathrm{d}s}\right)\right\rangle && (25)\\
s_z^{-1} &= 2ec_- + \partial_\delta \eta = \frac{1}{pv}\left\langle D_y \frac{\partial}{\partial y}\left(\frac{\mathrm{d}E}{\mathrm{d}s}\right) + \frac{\partial}{\partial \delta}\left(\frac{\mathrm{d}E}{\mathrm{d}s}\right)\right\rangle && (26)\\
\varepsilon_s^{eq} &= \chi_s s_s = \frac{E\beta^2}{2}\left\langle \frac{\beta_T \left(\frac{13.6\mathrm{MeV}}{pv}\right)^2 \frac{1}{X_0} + \mathcal{H}_s \langle\delta^2\rangle}{\frac{\mathrm{d}E}{\mathrm{d}s} - \frac{D_y}{2}\frac{\partial}{\partial y}\left(\frac{\mathrm{d}E}{\mathrm{d}s}\right)}\right\rangle && (27)\\
\varepsilon_z^{eq} &= \chi_z s_z = \frac{E\beta^2}{2}\left\langle \frac{\beta_L \langle\delta^2\rangle + \gamma_L D_y^2 \left(\frac{13.6\mathrm{MeV}}{pv}\right)^2 \frac{1}{X_0}}{D_y \frac{\partial}{\partial y}\left(\frac{\mathrm{d}E}{\mathrm{d}s}\right) + \frac{\partial}{\partial \delta}\left(\frac{\mathrm{d}E}{\mathrm{d}s}\right)}\right\rangle && (28)
\end{aligned}
$$

Both (25) and (26) have the dimension of an inverse length, as they should. Both (27) and (28) have the dimension of a length, if β_T, $\mathcal{H}_s$, β_L, and γ_L have the dimension of a length. I recall that in this section, the subscripts s and z mark the transverse and longitudinal motion, respectively.

3.4 Comparison of the Results of Neuffer and Wang and Kim

In Sections 3.4.1 and 3.4.2, I give the relations between Neuffer's longitudinal β-function $\beta_\parallel$ and longitudinal emittance $\varepsilon_\parallel$ and their standard definitions in MAD [7]. I then compare the results of

Neuffer and Wang and Kim in detail. In Section 3.4.3, I compare the transverse damping rates, show that the second term in the square bracket of (25) is half of the corresponding term in $g_\perp$ below (5), and give the reason. I derive in Section 3.4.4 on the longitudinal damping rate, that (26) agrees with (7). In Section 3.4.5, my result for the variation of the energy loss with energy in Section 3.4.5 agrees with Neuffer's result (10). My results for the emittances in Sections 3.4.6 and 3.4.7 confirm that Neuffer uses normalised emittances, while Wang and Kim use geometrical ones.

3.4.1 Definition of the Longitudinal β-Function

The goal of this section is finding the relation between Neuffer's longitudinal β-function (8), and standard definitions. MAD [7] computes α, β and γ functions in all three directions from the linear 6D map R for one turn with the EMIT command. If R is 2×2 block-diagonal, one can also calculate the α, β and γ functions by hand. I write for the linear longitudinal map $\mathcal{M}$ for an arc followed by an RF station, operating on the column vector $(ct, \delta p/p)^T$:

$$\mathcal{M} = \begin{pmatrix} 1 & \frac{ch\eta}{f_{\rm RF}\beta} \\ \frac{2\pi f_{\rm RF} eV\cos\varphi_s}{Ec\beta} & 1 + \frac{2\pi\eta heV\cos\varphi_s}{E\beta^2} \end{pmatrix} \tag{29}$$

Here, $f_{\rm RF}$ is the RF frequency, and the origin of the stable phase angle φ_s is at the last zero crossing of the RF voltage V. From (29) one finds to lowest order in the synchrotron tune Q_s in agreement with [8, 9]:

$$Q_s = \sqrt{-\frac{\eta heV\cos\varphi_s}{2\pi\beta^2 E}} \tag{30}$$

$$\beta_s = \frac{c}{f_{\rm RF}}\sqrt{-\frac{\eta hE}{2\pi eV\cos\varphi_s}} = \sqrt{-\frac{c\eta CE}{2\pi\beta f_{\rm RF} eV\cos\varphi_s}} \tag{31}$$

The longitudinal motion is stable, and Q_s is real and positive, if the product $\eta\cos\varphi_s < 0$. Hence, we need $0 \le \varphi_s < \pi/2$ below transition with $\eta < 0$, while we need $\pi/2 < \varphi_s \le \pi$ above transition with $\eta > 0$. It follows that (8) must be multiplied by $c\beta E/(2\pi f_{\rm RF})$ to obtain (31), remembering that the origin of φ_s in (8) is at the crest of the RF wave, and that $\sin(\varphi_s - \pi/2) = -\cos\varphi_s$.

$$\beta_s = \frac{c\beta E}{2\pi f_{\rm RF}}\beta_\parallel \tag{32}$$

Here, the factor $c\beta/(2\pi f_{\rm RF})$ converts the longitudinal coordinate from RF phase to scaled time ct, and the factor E converts the normalised β-function to the geometrical one. Note that β_s has the dimension of length, the same as the transverse β-functions.

3.4.2 Definition of the Longitudinal Emittance

The standard definitions of the normalised longitudinal emittance ε_s in units of m, and of ε_t in units of eVs are:

$$\varepsilon_s = \sqrt{\langle(c\Delta t)^2\rangle\langle(\Delta E/(E_\mu))^2\rangle} \tag{33}$$

$$\varepsilon_t = \sqrt{\langle(\Delta t)^2\rangle\langle(\Delta E)^2\rangle} \tag{34}$$

Here I neglect the cross correlation term $\langle(c\Delta t)(\Delta E/(E_\mu)\rangle$. Neuffer's definition of $\varepsilon_\parallel$ contains $\Delta\varphi$ instead of Δt or $c\Delta t$. It has the dimension of an energy. Hence, ε_s and ε_t are related to $\varepsilon_\parallel$ by:

$$\varepsilon_s = \frac{\lambda_{\mathrm{RF}}\varepsilon_\parallel}{2\pi E_\mu} \tag{35}$$

$$\varepsilon_t = \frac{\varepsilon_\parallel}{2\pi f_{\mathrm{RF}}} \tag{36}$$

The ratio $\varepsilon_s/\varepsilon_t = c/E_\mu$ is numerically 2.8374 m/eVs. Using (32), and (35) or (36), we can express (12) in terms of β_s:

$$\varepsilon_s^{eq} = \left(\frac{\mathrm{d}E}{\mathrm{d}s}\right)^{-1} \frac{\beta\beta_s}{2E_\mu g_\parallel} \frac{\mathrm{d}\langle\Delta E^2\rangle}{\mathrm{d}s} \tag{37}$$

$$\varepsilon_t^{eq} = \left(\frac{\mathrm{d}E}{\mathrm{d}s}\right)^{-1} \frac{\beta\beta_s}{2cg_\parallel} \frac{\mathrm{d}\langle\Delta E^2\rangle}{\mathrm{d}s} \tag{38}$$

3.4.3 Transverse Damping Rate

With minimal changes of notation, Neuffer's partition number $g_\perp$ can be written:

$$g_\perp = 1 - D_y \frac{\frac{\partial}{\partial y}\left(\frac{\mathrm{d}E}{\mathrm{d}s}\right)}{\frac{\mathrm{d}E}{\mathrm{d}s}} \tag{39}$$

Inserting (39) into (14), and using $\beta^2 E = pv$, brings $s_\perp^c$ into the form:

$$(s_\perp^c)^{-1} = \frac{1}{pv}\left[\frac{\mathrm{d}E}{\mathrm{d}s} - D_y \frac{\partial}{\partial y}\left(\frac{\mathrm{d}E}{\mathrm{d}s}\right)\right] \tag{40}$$

This agrees with the Wang and Kim result (25), apart from the wedge term proportional to D_y, which is twice as large. This discrepancy is due to Neuffer treating a quadrupole channel, and Wang and Kim treating a solenoid channel with $x - y$ exchange symmetry. In the latter case, transverse cooling is divided equally between the symmetrical and asymmetrical modes. The factor one half in (25) is also absent in Wang and Kim's treatment of a quadrupole channel [10].

3.4.4 Longitudinal Damping Rate

With minimal changes of notation, Neuffer's partition number $g_\parallel$ can be written:

$$g_\parallel = \frac{\frac{\partial}{\partial E}\left(\frac{\mathrm{d}E}{\mathrm{d}s}\right)}{\frac{\frac{\mathrm{d}p}{\mathrm{d}s}}{p}} + D_y \frac{\frac{\partial}{\partial y}\left(\frac{\mathrm{d}E}{\mathrm{d}s}\right)}{\frac{\mathrm{d}E}{\mathrm{d}s}} \tag{41}$$

The first term is related to the variation of the energy loss with energy. The second term is related to the wedges, and already in the form of the first term in (26). I introduce intermediate variables into the first term in (41) and write:

$$g_\parallel = p \frac{\frac{\partial}{\partial \delta}\left(\frac{\mathrm{d}E}{\mathrm{d}s}\right)\frac{\mathrm{d}\delta}{\mathrm{d}E}}{\frac{\mathrm{d}p}{\mathrm{d}E}\frac{\mathrm{d}E}{\mathrm{d}s}} + D_y \frac{\frac{\partial}{\partial y}\left(\frac{\mathrm{d}E}{\mathrm{d}s}\right)}{\frac{\mathrm{d}E}{\mathrm{d}s}} \tag{42}$$

As in [3], $\delta = (p - p_0)/p_0$ is the relative momentum error, p_0 is the nominal momentum, and E_μ is the rest energy of the muons. With the relativistic equations $\frac{\mathrm{d}\delta}{\mathrm{d}E} = \frac{1}{\gamma E_\mu}$, $\frac{\mathrm{d}p}{\mathrm{d}E} = \frac{1}{c\beta}$, $pc = \beta\gamma E_\mu$ we get:

$$g_\parallel = \frac{\frac{\partial}{\partial\delta}\left(\frac{\mathrm{d}E}{\mathrm{d}s}\right)}{\frac{\mathrm{d}E}{\mathrm{d}s}} + D_y \frac{\frac{\partial}{\partial y}\left(\frac{\mathrm{d}E}{\mathrm{d}s}\right)}{\frac{\mathrm{d}E}{\mathrm{d}s}} \tag{43}$$

Using (43) and $\beta^2 E = pv$ in (14) yields:

$$(s_\parallel^c)^{-1} = \frac{1}{pv}\left[\frac{\partial}{\partial\delta}\left(\frac{\mathrm{d}E}{\mathrm{d}s}\right) + D_y \frac{\partial}{\partial y}\left(\frac{\mathrm{d}E}{\mathrm{d}s}\right)\right] \tag{44}$$

The result (44) agrees with (26).

3.4.5 Variation of Energy Loss with Energy

With $\mathcal{A} = 4\pi N_A r_e^2 m_e c^2 \rho Z/A$, Neuffer writes for the rate of energy loss, neglecting the density effect by putting $\delta = 0$:

$$\frac{\mathrm{d}E}{\mathrm{d}s} = \mathcal{A}\left[\beta^{-2}\log(K\beta^2\gamma^2) - 1\right] \tag{45}$$

Writing (45) as a function of $\beta\gamma$ and constants, I find for

$$\frac{\partial}{\partial\beta\gamma}\left(\frac{\mathrm{d}E}{\mathrm{d}s}\right) = \frac{2\mathcal{A}\left(\gamma^2 - \log[K\beta^2\gamma^2]\right)}{\beta^3\gamma^3} \tag{46}$$

The partial derivative with respect to δ, needed in (42) to (44), is $\beta\gamma$ times larger than (46). The ratio of $\beta\gamma$ times (46) and (45), needed in (43), is:

$$\frac{\frac{\partial}{\partial\delta}\left(\frac{\mathrm{d}E}{\mathrm{d}s}\right)}{\frac{\mathrm{d}E}{\mathrm{d}s}} = \frac{2\left[\gamma^2 - \log K(\gamma^2-1)\right]}{\left[\gamma^2\log K(\gamma^2-1) - (\gamma^2-1)\right]} \tag{47}$$

The result (47) agrees with Neuffer's (9). For muons with $p = 200$ MeV/c in liquid hydrogen, it is numerically -0.294874. It vanishes at $p = 377.6$ MeV/c.

3.4.6 Transverse Equilibrium Emittance

With little effort, (11) can be brought into the form:

$$\varepsilon_\perp^{eq} = \frac{\beta^3\gamma E}{2}\left(\frac{\beta_\perp\left(\frac{13.6\mathrm{MeV}}{pv}\right)^2\frac{1}{X_0}}{\frac{\mathrm{d}E}{\mathrm{d}s} - D_y\frac{\partial}{\partial y}\left(\frac{\mathrm{d}E}{\mathrm{d}s}\right)}\right) \tag{48}$$

Comparing (48) to (27) shows four things: (i) The heating term $\mathcal{H}_s\langle\delta^2\rangle$ due to the coupling of the energy straggling to the betatron oscillations is absent. Neuffer [11] has shown that it is small compared to the cooling term in a typical cooling channel. In Section 5.2, I shall derive the conditions for this also to be true in my designs. (ii) There is an extra factor $\beta\gamma$ in front of the large brackets. This is consistent with Neuffer using normalised emittances and Wang and Kim using geometrical ones. (iii) The wedge term is multiplied by D_y instead of $D_y/2$. We have seen this factor already in (40), and discussed it in Section 3.4.3. (iv) The remaining coefficients in the large brackets agree, if β_T and $\mathcal{H}_s$ are the usual transverse amplitude functions $\beta_\perp$ and $\mathcal{H}$.

3.4.7 Longitudinal Equilibrium Emittance

My version of Neuffer's equation for the longitudinal equilibrium emittance (37) can be brought into the form:

$$\varepsilon_s^{eq} = \frac{\beta\gamma E}{2}\left(\frac{\beta_s \frac{\mathrm{d}\langle(\Delta E/E)^2\rangle}{\mathrm{d}s}}{\frac{\partial}{\partial\delta}\left(\frac{\mathrm{d}E}{\mathrm{d}s}\right) + D\frac{\partial}{\partial y}\left(\frac{\mathrm{d}E}{\mathrm{d}s}\right)}\right) \tag{49}$$

Remembering, that $\Delta E/E = \beta^2\Delta p/p$ and that the Wang and Kim parameter $\langle\delta^2\rangle$ is the rate of change per unit length of the relative momentum error, we see that the factor in front of the large brackets agrees with Wang and Kim's (28), with the understanding that Neuffer and I use normalised emittances, and Wang and King use geometrical ones. The denominators in the large brackets agree too. In the numerator between the large brackets in (49), the heating term due to multiple scattering, the second term in Wang and Kim's (28) is absent. In Section 5.2, I shall derive the condition for it to be small compared to the cooling term. Apart from this discrepancy, (49) and (28) agree, if the dimension of β_L is metres as that of D_y, β_s and X_0, and the dimension of γ_L is inverse metres as that of γ_s.

4 PUBLISHED COOLING CHANNELS

In this chapter I apply the equations to some published cooling channels. Tab. 2 shows the results. The first two columns refer to the purely transverse cooling channels in Study I [4] and Study II [5], respectively. I can use the formulae in Chapter 2. The cooling channel in Study I has two absorbers in a lattice period. The cooling channel in Study II is "tapered". The transverse amplitude function varies from about 0.35 m to about 0.18 m, while the period length changes from 2.75 m to 1.65 m. I use the values at the end. The third column shows the parameters of a ring cooler, designed by Balbekov [6], that cools both transversely and longitudinally. It uses liquid hydrogen absorbers in dispersion-free regions for transverse cooling, and wedge shaped LiH absorbers, which occupy half of the vertical aperture, in regions with vertical dispersion for longitudinal cooling. At least for Study I, the merit factor M, calculated from (4), is quite misleading, since it ignores the severe muon losses at the beginning of the cooling channel.

5 COOLING CHANNEL DESIGN PARAMETERS

Our goal is finding a practicable design for a cooling channel that cools a muon beam with assumed initial to assumed final emittances. The former are determined by the properties of the muon collection system, the latter by those of the muon acceleration and storage systems. The equilibrium emittances should be smaller than the final ones by a good factor, as shown in Chapter 2. Compromises on this goal should only be considered, once unsurmountable difficulties have been encountered in the design of a real cooling channel.

As an application I use cooling channels with parameters shown in Tab. 3. The nominal channel is in column 1. It is supposed to cool a muon beam with parameters corresponding to Study II parameters at 186 m from the source [12] to transverse parameters similar to those in Study II, and in addition to cool longitudinally by a factor of three in emittance. Remember that the transverse equilibrium emittance in a cooling channel, which cools both transversely and longitudinally, is

Table 2: Parameters of published cooling channels. The radiation length X_0 is for liquid hydrogen absorbers without windows. Windows on absorbers and RF cavities reduce X_0 and increase the equilibrium emittances. The channel length and the final emittances of the ring cooler are shown for 15 turns.

Parameter	Study I	Study II	Ring
Muon momentum p/MeV/c	200	200	225.6
Period length L_P/m	2.2	1.65	18.5
Channel length S/m	165	107.8	554.4
Straight liquid H_2 Absorber			
Absorber length L_A/m	2·0.126	0.21	1.28
Loss rate $\mathrm{d}E/\mathrm{d}s$/MeV/m	31.75	31.75	31.75
Radiation length X_0/m	8.66	8.66	8.66
Ampl. function $\beta_\perp$/m	0.35	0.18	0.26
Wedge LiH Wedge Absorber			
Absorber length L_W/m	–	–	0.14
Loss rate $\mathrm{d}^2E/\mathrm{d}s/\mathrm{d}y$/MeV/m^2	–	–	
Radiation length X_0/m	–	–	1.02
Ampl. function $\beta_\perp$/m	–	–	0.50
Dispersion D_y/m	–	–	0.47
Initial transv. emittance $\varepsilon_\perp^i$/mm	15	12	12
Final transv. emittance $\varepsilon_\perp^f$/mm	2	2.7	2.1
Equil. transv. emittance $\varepsilon_\perp^{eq}$/mm	1.26	0.648	
Transv. cooling length $s_\perp^c$/m	56.5	63.0	
Initial long. emittance $\varepsilon_\parallel^i$/mm	–	–	15
Final long. emittance $\varepsilon_\parallel^f$/mm	–	–	6.3
Equil. long. emittance $\varepsilon_\parallel^{eq}$/mm	–	–	
Long. cooling length $s_\parallel^c$/m	–	–	
Merit factor M	49.3	18.1	

about a factor of two larger than that in a channel that cools only transversely. I assume that the channel length is $S = 200$ m. Here S is the length of an open channel, or the product of circumference and number of turns of a ring cooler. The remaining columns show the consequences of varying the input parameters. The input parameters in the upper part of Tab. 3 are the starting point for my design procedure that is written as a *Mathematica* notebook. In order to achieve the design parameters, the cooling channel must have the parameters in the lower part of Tab. 3 which I shall now derive.

In this first round of the design procedure, I use Neuffer's equations that apply to a quadrupole cooling channel, and neglect the extra cross-plane heating terms in Wang and Kim's equations, due to dispersion at the wedge-shaped absorbers. However, I use a comparison of the heating terms to derive upper limits for the vertical dispersion at the wedge absorbers.

Table 3: Parameters of cooling channels. The nominal channel is in column 1. The other columns show variants. Parameters that apply to both horizontal and vertical motion are labelled transverse and have a subscript $\perp$. Parameters that apply only to the horizontal or vertical plane are labelled horizontal or vertical and have a subscript h or v. Longitudinal parameters have a subscript $\|$. At the wedge absorbers, $D_x = 0$ and $D_y \neq 0$. Slip factor and RF frequency are listed at the intersection of the limits due to β_s and bucket height $b_{RF} = 2\Delta p/p = 0.2$. The stable phase angle is $\varphi_s = 2\pi/3$. Input parameters are above the horizontal line. Calculated parameters are below it.

Column	1	2	3	4	5	
Muon momentum p	200	200	200	200	200	MeV/c
Initial transv. emittance $\varepsilon_\perp^i$	10	10	10	10	10	mm
Final vert. emittance ε_v^f	3	3	5	3	5	mm
Equil. vert. emittance ε_v^{eq}	1	1	2	1	2	mm
Initial long. emittance $\varepsilon_\|^i$	150	150	150	150	150	mm
Final long. emittance $\varepsilon_\|^f$	50	50	50	30	30	mm
Equil. long. emittance $\varepsilon_\|^{eq}$	15	15	15	10	10	mm
Channel length S	200	300	200	200	300	m
Vert. cooling length s_v^c	133	199	204	133	306	m
Long. cooling length $s_\|^c$	148	222	148	103	154	m
Vert. partition number g_v	0.372	0.372	0.297	0.307	0.236	
Wedge parameter $D_y\ell'/\ell_0$	0.628	0.628	0.703	0.693	0.764	
Hor. cooling length s_h^c	49.4	74.1	60.5	40.9	72.3	m
Equil. hor. emittance ε_h^{eq}	0.372	0.372	0.593	0.307	0.473	mm
Final hor. emittance ε_h^f	0.540	0.540	0.939	0.380	0.623	mm
Long. partition number $g_\|$	0.334	0.334	0.408	0.398	0.469	
Average acceleration $\langle\frac{\mathrm{d}E}{\mathrm{d}s}\rangle$	3.6	2.4	2.9	4.3	2.4	MeV/m
Absorber occupancy factor	11.3	7.5	9.2	13.6	7.7	%
Transv. β-function $\beta_\perp$	103	103	165	85.4	131	mm
Length of absorbers L_A	206	206	330	171	263	mm
Channel period length L_P	1.83	2.75	3.58	1.25	3.41	m
Init. hor. beam radius σ_x^i	23.4	23.4	29.5	21.2	26.3	mm
Init. hor. divergence $\sigma_x^{i\prime}$	226	226	179	249	201	mr
Straggling rate $\mathrm{d}\langle\Delta E^2\rangle/\mathrm{d}s$	3.3	3.3	3.3	3.3	3.3	MeV^2/m
Long. β-function β_s	11.5	11.5	14.1	9.14	10.8	m
Min. dispersion $\|D_y\|$	44	44	62	44	60	mm
Max. dispersion $\|D_y\|$	297	297	474	246	378	mm
Slip factor η	0.320	0.214	0.320	0.308	0.205	
RF frequency f_{RF}	14.3	14.3	11.7	18.0	15.3	MHz
Merit factor M	158	146	54.5	373	126	

5.1 Cooling Lengths and Partition Numbers

I assume as before that the horizontal dispersion D_x vanishes at the absorbers, while the vertical dispersion D_y does not. Then the vertical and longitudinal partition numbers are $0 < g_v, g_\parallel < 1$, while the horizontal partition number g_h is always unity [2]. In the first step of my procedure, I get the vertical and longitudinal cooling lengths by solving (15) for s_v^c and $s_\parallel^c$, respectively:

$$s_v^c = S \log \frac{\varepsilon_\perp^i - \varepsilon_v^{eq}}{\varepsilon_v^f - \varepsilon_v^{eq}} \qquad\qquad s_\parallel^c = S \log \frac{\varepsilon_\parallel^i - \varepsilon_\parallel^{eq}}{\varepsilon_\parallel^f - \varepsilon_\parallel^{eq}} \tag{50}$$

The cooling lengths are proportional to the channel length S, and have a logarithmic dependence on the initial, final, and equilibrium emittances. I use Neuffer's result (13) and (14), that the product of cooling length and partition number is the same in both planes, to obtain the partition numbers g_v and $g_\parallel$, and hence the wedge parameter $D\ell'/\ell_0 = 1 - g_v$.

Since $g_h = 1$, both the horizontal cooling length s_h^c and the horizontal equilibrium emittance ε_h^{eq} are g_v times smaller than the vertical ones. The final horizontal emittance, obtained from (15), is even smaller than the vertical equilibrium emittance. Hence, the two transverse emittances will be different at the end of the cooling channel if they are equal at its beginning, and if the horizontal and vertical β-functions at the absorber are also the same. It is possible to achieve $\varepsilon_h^f \approx \varepsilon_v^f$, by making horizontal cooling less efficient, and using $\beta_h > \beta_\perp$, and hence $\varepsilon_h^{eq} > \varepsilon_v^{eq}$.

The cooling lengths lead directly to the average rate of energy loss in the absorbers $\langle \mathrm{d}E/\mathrm{d}s \rangle$, by solving (13) and (14). In order to get the cooling lengths listed, the average rate of energy loss is about 2.5 MeV/m. For given emittances, the average rate of energy loss is inversely proportional to the channel length.

5.2 Amplitude Functions and Dispersion

We get an upper limit of the vertical amplitude function at the absorbers $\beta_\perp$ due to the transverse equilibrium emittance by solving (11):

$$\beta_\perp \leq \frac{2\beta g_\perp E_\mu X_0 \varepsilon_\perp^{eq}}{(13.6\mathrm{MeV})^2} \left(\frac{\mathrm{d}E}{\mathrm{d}s} \right) \tag{51}$$

From the parameters of the absorber, we can calculate the mean square energy variation $\mathrm{d}\langle \Delta E^2 \rangle / \mathrm{d}s$ due to straggling, using (9), and an upper limit for the longitudinal amplitude function β_s due to the longitudinal equilibrium emittance, using (37):

$$\beta_s \leq \frac{2E_\mu g_\parallel \varepsilon_s^{eq}}{\beta} \left(\frac{\frac{\mathrm{d}E}{\mathrm{d}s}}{\frac{\mathrm{d}\langle \Delta E^2 \rangle}{\mathrm{d}s}} \right) \tag{52}$$

The fraction in the large brackets depends only on the absorber material. The amplitude functions $\beta_\perp$ and β_s, and the length L_A of the absorber are essentially proportional to the products of partition number and equilibrium emittance $g\varepsilon^{eq}$.

The absolute value of the vertical dispersion $|D_y|$ at the absorbers has a lower limit due to the wedge parameter, since it would be nice if the absorber length were positive in the whole vertical aperture. Taking an aperture radius equal to three RMS beam radii σ_y, I find:

$$|D_y| \geq 3(1 - g_v)\sigma_y = 3(1 - g_v)\sqrt{\varepsilon_\perp^i \beta_\perp / (\beta\gamma) + (D_y \sigma_e^i)^2} \tag{53}$$

Here σ_e^i is the initial relative RMS momentum spread. Solving (53) for $|D_y|$ yields:

$$|D_y| \geq 3(1-g_v)\sqrt{\frac{\varepsilon_\perp^i \beta_\perp}{\beta\gamma[1-(3(1-g_v)\sigma_e^i)^2]}} \tag{54}$$

$|D_y|$ is real and positive if $3(1-g_v)\sigma_e^i \leq 1$. This condition is also found by assuming that σ_y is dominated by σ_e^i, and neglecting the contribution of the betatron oscillations. Upper limits to $|D_y|$ are due to the cross-plane heating terms of the equilibrium emittances (27) and (28). If the absorber is at a waist of the beam envelope with $\gamma_\perp = 1/\beta_\perp$ and $D_y' = 0$, we have $\mathcal{H} = D_y^2/\beta_\perp$. Hence, the heating term due to energy straggling is smaller than or equal to the heating term due to multiple scattering in (27), if the following condition holds:

$$|D_y| \leq \frac{\beta_\perp(13.6\mathrm{MeV}/pv)}{\sqrt{X_0\langle\delta^2\rangle}} \tag{55}$$

Applying a similar argument to (28), the heating term due to multiple scattering is smaller than or equal to the heating term due to energy straggling, if $|D_y|$ satisfies:

$$|D_y| \leq \frac{\beta_s\sqrt{X_0\langle\delta^2\rangle}}{(13.6\mathrm{MeV}/pv)} \tag{56}$$

I recall that, in (55) and (56), $\langle\delta^2\rangle$ is the rate of change per unit of length of the relative momentum error due to straggling. Tab. 3 shows the limits from (54) and (55). The limit from (56) is much higher. When D_y is one half of (55) or (56), then the cross-plane heating term contributes one quarter of the in-plane heating term to the equilibrium emittance.

5.3 Absorbers

I assume that there is one kind of wedge-shaped, liquid hydrogen absorber with a loss rate $\mathrm{d}E/\mathrm{d}s = 31.75$ MeV/m and a radiation length $X_0 = 8.66$ m. The absorber occupancy factor is simply the ratio of $\langle\mathrm{d}E/\mathrm{d}s\rangle$ and the assumed rate of energy loss $\mathrm{d}E/\mathrm{d}s$ in the absorber. The length of an individual absorber L_A should not be larger than $2\beta_\perp$, in order to limit the value of the β-function at the ends of the absorber to be at most $2\beta_\perp$. Dividing L_A by the absorber occupancy factor yields an upper limit for the spacing between neighbouring absorbers, and hence the length of a period L_P in the cooling channel. An obvious improvement of the theory would be replacing $\beta_\perp$ by a suitable average over the length of the absorber. The arithmetic mean is $\langle\beta_\perp\rangle = 4\beta_\perp/3$.

The initial horizontal RMS beam radius σ_x and both divergences $\sigma_{x'}$ and $\sigma_{y'}$ at the centre of the absorber follow from the initial transverse emittance $\varepsilon_\perp^i$ and $\beta_\perp$, assuming that D_x, D_x' and D_y' vanish there:

$$\sigma_x = \sqrt{\frac{\varepsilon_\perp^i\beta_\perp}{\beta\gamma}} \qquad\qquad \sigma_{x'} = \sigma_{y'} = \sqrt{\frac{\varepsilon_\perp^i}{\beta\gamma\beta_\perp}} \tag{57}$$

The vertical dispersion D_y and the RMS momentum spread contribute to the vertical RMS beam σ_y. To get an upper limit for σ_y, one might use (55) and 1/3 of the bucket height. At either end of the absorber, σ_x is larger by a factor $\sqrt{2}$, while σ_y is larger by almost as much. Both $\sigma_{x'}$ and $\sigma_{y'}$ are not small compared to unity, invalidating the par-axial approximation in beam dynamics. Palmer reminded me that this is a generic feature of cooling channels with a factor as large as ten between initial and equilibrium transverse emittances and constant $\beta_\perp$. Tab. 3 shows σ_x and $\sigma_{x'}$.

5.4 RF System and Longitudinal Dynamics

The RF system must do three things: (i) Compensate the energy loss in the absorbers, (ii) achieve the assumed initial longitudinal equilibrium emittance by having a value of β_s that satisfies (52), (iii) have a bucket height large enough to accept the momentum spread in the beam, (iv) have a bucket area that matches or is smaller than the initial longitudinal emittance $\varepsilon_\parallel^i$. The average rate of acceleration in the RF cavities is equal to the average rate of energy loss $\langle \mathrm{d}E/\mathrm{d}s\rangle$, if the muon energies at the entrance and the exit of the cooling channel are the same. It was already derived in Section 5.3. The average voltage gradient inside the RF cavities is higher than the average rate of acceleration for two reasons: (i) The RF cavities occupy only a fraction of the channel length, and (ii) the peak voltage gradient is higher than the accelerating gradient when the muons are accelerated off the crest of the RF wave form.

The conditions on β_s and bucket area also involve the longitudinal dynamics, and include the slip factor η. Below, I avoid fixing the sign of η and the quadrant of φ_s by taking absolute values where needed. By suitably arranging (31), introducing the circumference C of the cooling ring, which will promptly drop out of the equations, and using $eV|\sin\varphi_s| = C\langle \mathrm{d}E/\mathrm{d}s\rangle$, we find for the ratio $|\eta|/f_{\mathrm{RF}}$, needed to satisfy the condition (52) on β_s:

$$\frac{|\eta|}{f_{\mathrm{RF}}} \leq \frac{2\pi\beta\beta_s^2\langle \mathrm{d}E/\mathrm{d}s\rangle}{cE\tan\varphi_s} \tag{58}$$

The second relation between η and f_{RF} follows from the requirement that the relative half bucket height b_{RF} is large enough to accept the relative RMS momentum spread in the beam $\Delta p/p$, assuming $b_{RF} = 2\Delta p/p$. The relation can be written in the form:

$$f_{\mathrm{RF}}|\eta| = \frac{Y^2(\varphi_s)}{\sin\varphi_s}\frac{\langle \mathrm{d}E/\mathrm{d}s\rangle c}{4\pi\beta E}\left(\frac{\Delta p}{p}\right)^{-2} \tag{59}$$

Here $Y(\varphi) = \sqrt{|(\pi - 2\varphi)\sin\varphi - 2\cos\varphi|}$ with $Y(0) = \sqrt{2}$ describes the dependence of b_{RF} on the stable phase angle φ. Fig. 1 shows the upper limits for the absolute value of the slip factor η as a function of the RF frequency f_{RF}, caused by β_s from (58), and due to three bucket heights from (59) for $\varphi_s = 2\pi/3$. Doubling the bucket height reduces the values of $|\eta|$ and f_{RF} at the intersection by a factor of two.

A third relation between η and f_{RF} follows from the requirement that the bucket area is at least 4π times the initial longitudinal emittance $\varepsilon_\parallel^i$. The factor 4π might also be 6π or 9π. Remember that the traditional formula for the bunch area is the true area, while my definition of the emittance is the product of the standard deviations. Comparing emittance and bucket area implies that the bunches are matched to the buckets at the entrance to the cooling channel. If this is not true, a comparison between momentum spread and bucket height, or between bunch length and bucket length, is more appropriate. The relation can be written in the form:

$$|\eta| f_{\mathrm{RF}}^3 \leq \frac{2\alpha^2(\varphi_s - \pi/2)\langle \mathrm{d}E/\mathrm{d}s\rangle\gamma}{(\pi\varepsilon_\parallel^i)^2 E_\mu \sin\varphi_s}\left(\frac{\beta c}{\pi}\right)^3 \tag{60}$$

Here, $\alpha(\psi)$ is a bucket area function, with the origin of ψ at the crest of the RF wave, and $\alpha(0) = 0$ and $\alpha(\pi/2) = 1$. Dôme [13] gives a series expansion for $\alpha(\psi)$. Fig. 2 shows it.

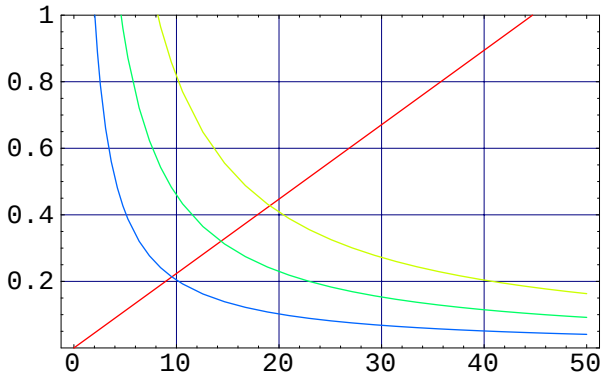

Figure 1: Upper limits for the slip factor $|\eta|$ as function of RF frequency in MHz at $\varphi_s = 2\pi/3$. The straight red curve shows the limit due to β_s. The yellow, green and blue hyperbolic curves from above show the limits for relative RMS momentum spreads $\Delta p/p = 0.075, 0.1, 0.15$.

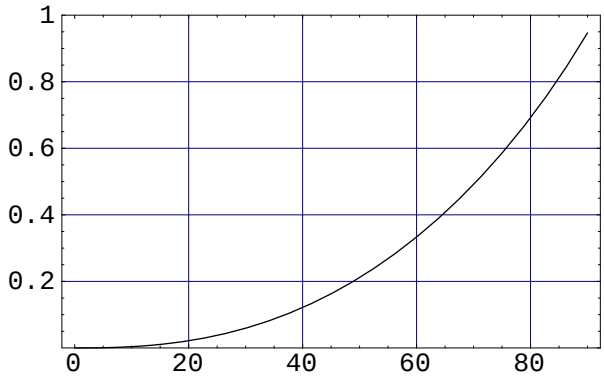

Figure 2: Bucket area function $\alpha(\psi)$ as a function of ψ in degrees. The origin of ψ is at the crest of the RF wave. At $\psi = 90^\circ$ the value should be unity. The difference is caused by the series expansion.

$$\alpha(\psi) = \frac{3|\psi|^{5/2}}{10}\left[1 - \frac{1}{15}\left(\frac{\psi}{2}\right)^2 + \frac{1607}{19110}\left(\frac{\psi}{2}\right)^4 + \frac{939031}{12370050}\left(\frac{\psi}{2}\right)^6 + \frac{397918669}{4855851000}\left(\frac{\psi}{2}\right)^8 + \ldots\right] \tag{61}$$

Fig. 3 shows the upper limits for the absolute value of the slip factor η as a function of the RF frequency $f_{\rm RF}$ for $\varphi_s = 2\pi/3$, due to β_s from (58), and due to three bucket areas from (60). Increasing the bucket area in the ratio 9/4 reduces the values of $|\eta|$ and $f_{\rm RF}$ at the intersection by a factor $3/2 = \sqrt{9/4}$. Fig. 4 shows the upper limits for $|\eta|$ as a function of the RF frequency $f_{\rm RF}$ for three stable phase angles $\varphi_s = 5\pi/6, 3\pi/4, 2\pi/3$, due to β_s from (58), and due to a bucket area 1.35π m from (60). Reducing the stable phase angle from $5\pi/6$ to $2\pi/3$, and reducing the peak RF voltage in the ratio $\sqrt{3}$, reduces $|\eta|$ by about a factor 6 and $f_{\rm RF}$ by about a factor 3/2. I do not necessarily propose to operate a muon cooling channel at values of $|\eta|$ and $f_{\rm RF}$ where the limiting curves intersect. I simply take them as a starting point for scaling. Doubling $f_{\rm RF}$ reduces $|\eta|$ by a factor of eight when the bucket area is the limit, and by a factor of two when the bucket height is the limit.

The relative bucket height $b_{\rm RF}$ in Tab. 3 is 0.2 for the nominal cooling channel. Hence, at the nominal values of $|\eta|$ and $f_{\rm RF}$ muons with momenta between 160 and 240 MeV/c are inside the bucket. If this range is not considered large enough, the RF system must be operated at a higher frequency. If $f_{\rm RF}$ is scaled up at constant bucket area and constant stable phase angle φ_s, the bucket height is proportional to $f_{\rm RF}$. I repeat that constant bucket area implies scaling $|\eta|$ down like $1/f_{\rm RF}^3$.

The maximum permissible value of the absolute value of the slip factor $|\eta|$ as a function of the RF frequency $f_{\rm RF}$ is given by up to three phenomena: (i) at low $f_{\rm RF}$, $|\eta| \propto f_{\rm RF}$ is determined

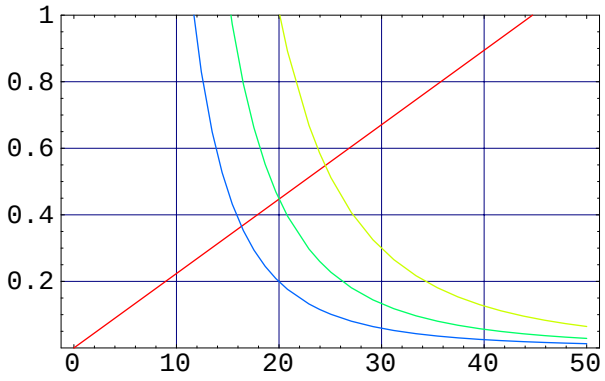

Figure 3: Upper limits for the slip factor $|\eta|$ as function of RF frequency in MHz at $\varphi_s = 2\pi/3$. The straight red curve shows the limit due to β_s. The yellow, green and blue hyperbolic curves from above show the limits for bucket areas 0.6π, 0.9π and 1.35π m.

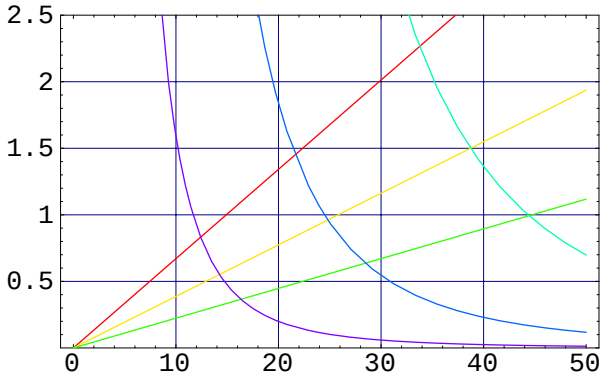

Figure 4: Upper limits for the slip factor $|\eta|$ as function of RF frequency in MHz for $\varphi_s = 5\pi/6, 3\pi/4, 2\pi/3$ from above. The straight curves show the limits due to β_s. The hyperbolic curves show the limits for a bucket area 1.35π m.

by β_s from (58); (ii) at high $f_{\rm RF}$, $|\eta| \propto f_{\rm RF}^{-3}$ is determined by the bucket area from (60); (iii) at intermediate values of $f_{\rm RF}$, $|\eta| \propto 1/f_{\rm RF}$ is determined by the bucket height from (59). Depending on the parameters of the cooling channel, this limit may be higher than the other two.

5.5 Merit Factor

The merit factor M is calculated from (4). It is meaningful only if losses along the channel for reasons other than muon decay are negligible compared to the decay losses.

6 DISCUSSION

In this chapter, I first discuss the consequences of changing one or more of my input parameters. Finding a lattice for a cooling channel, i.e. the precise arrangement of magnets, RF cavities, absorbers, etc., is well beyond the scope of this paper. However, I summarise in Section 6.2 the parameters that such a lattice must have in order to fulfil its purpose.

6.1 Consequences of Changes in Input Parameters

Tab. 3 shows the parameters of the nominal cooling channel in the first column. The other columns show the consequences of changing input parameters.

- The length of the cooling channel is increased in the second column. This increases the cooling lengths s_h^c, s_v^c, $s_\parallel^c$ and the channel period length L_P in the same proportion, and decreases the average acceleration $\langle {\rm d}E/{\rm d}s \rangle$, the absorber occupancy factor and the limit on the slip factor η in inverse proportion. The merit factor decreases because of the smaller fraction of surviving muons. The other parameters remain the same.

- The final and equilibrium values of the vertical emittance are increased in the third column. This increases the vertical cooling length, but leaves the longitudinal one unchanged. This is achieved by increasing the longitudinal partition number, and decreasing the vertical one. All changes of the other calculated parameters are a consequence. The most noticeable changes are the increases of $\beta_\perp$, L_A and L_P, and the reduction of M by almost a factor of three.

- The final and equilibrium values of the longitudinal emittance are decreased in the fourth column. This decreases the longitudinal cooling length, but leaves the vertical one unchanged. As in the third column, this is achieved by increasing the longitudinal partition number, and decreasing the vertical one. This channel is more difficult, having higher $\langle \mathrm{d}E/\mathrm{d}s \rangle$, absorber occupancy factor, and smaller $\beta_\perp$, L_A and L_P. Its merit factor M is more than twice that in the first column.

- The fifth column shows a cooling channel with all three previous changes combined, i.e. it is longer, and has less vertical and more longitudinal cooling than the nominal channel in the first column. All its parameters are "easier", but it still has almost the same merit factor M.

6.2 Lattice and RF System

The lattice transports and focuses the muon beam along the cooling channel. The RF system compensates the ionization loss in the absorbers and focuses the muon beam inside RF buckets. In order achieve the assumed performance, it must have the properties listed in Tab. 3:

- The β-functions at the absorber $\beta_\perp$ and β_s must not be larger than those derived in (51) and (52), in order to achieve the assumed equilibrium emittances.

- The horizontal dispersion $D_x = 0$ at the absorber must vanish, and the absolute value of the vertical dispersion $|D_y|$ must be within the limits (54) and (55), in order to achieve a positive absorber length across the vertical aperture, and to avoid excessive cross-plane heating, and the associated increase in the equilibrium emittances.

- The wedge-shaped liquid hydrogen absorbers must have length L_A and wedge parameter $D_y \ell'/\ell_0$ as shown in Tab. 3. Their spacing must be smaller than or equal to L_P.

- The lattice must provide the space for the RF system that makes up for the energy loss in the absorbers. At a stable phase angle $\varphi_s = 2\pi/3$, the average peak voltage gradient of the channels in Tab. 3 is at least between 2.1 and 3.9 MV/m, assuming that the RF system occupies all the space not taken by the absorbers. Practically feasible RF voltage gradients determine the length of the cooling channel.

- The slip factor η and the RF frequency f_{RF} must provide a bucket area matched to the initial longitudinal emittance. This is achieved by the combination of $|\eta|$ and f_{RF} shown in Tab. 3. For higher values of f_{RF}, the bucket area is constant if the ratio $|\eta|/f_{\mathrm{RF}}^3$ is held constant. For every factor of two in f_{RF}, $|\eta|$ goes down by a factor of eight. At constant bucket area and constant stable phase angle, the bucket height, which determines the accepted momentum range, is proportional to f_{RF}.

7 CONCLUSIONS

A procedure was developed for the calculation of parameters for muon cooling channels that achieve a prescribed performance. It is meant to be used as the first step in the design proper of such a channel, which finds an arrangement of practical magnets, RF cavities and absorbers that meets the required parameters.

The procedure is written in *Mathematica* . It starts with assumed values for initial, final and equilibrium beam emittances, material properties of the absorbers for ionization cooling, and the length of the channel. It derives first the e-folding lengths for ionization cooling in the vertical, horizontal and longitudinal direction, and the associated partition numbers. It finds upper limits for the transverse and longitudinal amplitude functions at the absorbers, and uses them to determine absorber parameters such a length, aperture radius, wedge parameter, and spacing between neighbouring absorbers. A finite value of the dispersion, assumed to be in the vertical direction, is needed to achieve both transverse and longitudinal cooling. The procedure calculates lower and lower limits for its absolute value. The RF system compensates the muon energy loss in the absorbers, and occupies most of the space between them. Relations between its parameters, such as frequency f_{RF}, stable phase angle φ_s, bucket area and height, lattice parameters such as the absolute value of the slip factor η, and muon beam parameters such as longitudinal emittance $\varepsilon_{\parallel}$ are used to find consistent parameter sets which are the starting point for further scaling. The scaling laws are given.

The procedure is first applied to find the parameter of a "nominal" muon cooling channel. The consequences of changing the input parameters a few at a time are presented. They indicate the changes needed to make cooling channels "easier" to build without compromising their performance. Further explorations of parameter space can be done very quickly.

Acknowledgements

I thank David Neuffer and Chun-xi Wang for helpful discussions.

References

[1] C.M. Ankenbrandt et al., Status of muon collider research and development and future plans, Phys.Rev. ST Accel.Beams **2** (1999) 081001 and references therein

[2] D. Neuffer, Calculation of Predicted Performance for Muon Cooling Rings, MUCOOL Note 227.

[3] C.-x. Wang and K.-J. Kim, Linear theory of ionization cooling in 6D phase space, Phys. Rev. Lett. **88** (2002) 184801, also MUCOOL Note 240 (2002).

[4] N. Holtkamp and D. Finley (eds.), A Feasibility Study of a Neutrino Source Based on a Muon Storage Ring, FERMILAB-PUB-00-108-E (2000).

[5] S. Ozaki, R. Palmer, M. Zisman and J. Gallardo (eds.), Feasibility Study-II of a Muon Based Neutrino Source, BNL-52623 (2001), also available at http://www.cap.bnl.gov/mumu/studyii/

[6] V. Balbekov, Ring Cooler Progress, MUCOOL Note 246 (2002).

[7] H. Grote and F.C. Iselin, The MAD Program, Version 8.16, User's Reference Manual, CERN SL/90-13 (AP) Rev.4 (1995).

[8] H. Wiedemann, Particle Accelerator Physics I (Springer, Berlin 1999) 275.

[9] D.A. Edwards and M. Syphers in: A.W. Chao and M. Tigner (eds.), Handbook of Accelerator Physics and Engineering (World Scientific, River Edge 1999) 51.

[10] C.-x. Wang and K.-J. Kim, Linear theory of transverse and longitudinal ionization cooling in a quadrupole channel, MUCOOL Note 222 (2001).

[11] D. Neuffer, Transverse Emittance Increase by Energy-Loss Straggling and Dispersion, MUCOOL Note 243 (2002).

[12] R. Fernow, private communication.

[13] G. Dôme, Theory of RF Acceleration, in: CERN 87-03 (1987) 110.